sustainability

MDPI

Article

Spatiotemporal Evolution of Ecological Patterns and Ecological-Security Risk Assessment with Identification of Potential Influencing Factors in the Agro-Pastoral Ecotone of Inner Mongolia

Ziyue Zhang [1,2], Long Ma [1,2,*], Bolin Sun [1,2,*], Xing Huang [1,2], Qiang Zhang [3], Chenyue Wang [1,2] and Jiamei Yuan [1,2]

[1] State Key Laboratory of Water Engineering Ecology and Environment in Arid Area, Inner Mongolia Agricultural University, Hohhot 010018, China; zhangziyue@emails.imau.edu.cn (Z.Z.)
[2] Inner Mongolia Key Laboratory of Ecohydrology and High-Efficient Utilization of Water Resources, Hohhot 010018, China
[3] Guangdong Provincial Key Laboratory of Wastewater Information Analysis and Early Warning, School of Technology for Sustainability, Beijing Normal University, Zhuhai 519087, China
* Correspondence: malong@emails.imau.edu.cn (L.M.); bolin-sun@imau.edu.cn (B.S.)

Abstract

As an important ecologically sensitive zone and ecological security barrier in northern China, the agro-pastoral ecotone of Inner Mongolia has an ecological pattern and security status that are closely related to regional sustainable development. Based on satellite remote sensing, land-cover, and meteorological observation data from 2000 to 2023, this study applied an ecological pattern transition matrix, vegetation models, and the PSR framework to quantitatively analyze regional ecosystem transitions, ecological function evolution, and ecological security risks. The results showed that from 1990 to 2023, forest and grassland areas increased, desert, water body, and wetland areas decreased, and settlements exhibited a sharp expansion trend. From 2000 to 2023, the region exhibited an apparent warming tendency and a statistically significant wetting trend. NPP and NDVI displayed an increasing spatial distribution from northwest to southeast. For the independently observed NDVI, correlation with precipitation ($r = 0.823$) was markedly higher than with temperature ($r = 0.141$). Correlation coefficients for model-simulated NPP against climate variables should be interpreted with caution because precipitation and temperature are explicit inputs within the NPP empirical-statistical model. The ecological security index of the study area generally increased, while the response subsystem continued to decline after 2005. The security levels showed spatial differentiation characterized by security in the northeast, insecurity in the southwest, and critical status in the central region, and the areas showing improvement gradually expanded from 2000 to 2023. In addition, feasible and constructive ecological restoration and regulation strategies were proposed for different regions. This study reveals the evolutionary characteristics and potential influencing mechanisms of regional ecological patterns and security, providing support for the construction of the ecological security barrier in northern China.

Keywords: agro-pastoral ecotone of Inner Mongolia; ecological pattern transition; ecological function evolution; ecological security assessment

Check for updates

Academic Editor: Jeroen Meersmans

Received: 14 September 2026
Revised: 20 October 2026
Accepted: 21 October 2026
Published: 23 October 2026

Copyright: © 2026 by the authors. Licensee MDPI, Basel, Switzerland. This article is an open access article distributed under the terms and conditions of the Creative Commons Attribution (CC BY) license.

1. Introduction

The agro-pastoral ecotone of Inner Mongolia extends across northern China from northeast to southwest. It is the agro-pastoral ecotone with the largest area and the longest spatial span in China. It is not only a mosaic transition zone between agricultural and pastoral production modes, but also an intersection zone of multiple climate types, including cold-temperate, temperate, and semi-arid climates. Under the superimposed influence of multiple climate systems, the region experiences strong climatic fluctuations and has a highly sensitive ecological environment, making it a typical ecological sensitive zone and a key area of the ecological security barrier in northern China.

Internationally, research on ecosystem security and restoration started relatively early. In the 1920s, a team from the University of Wisconsin in the United States first proposed the concept of "land security" through grassland restoration experiments [1]. In the 1950s and 1960s, many countries around the world initiated ecological restoration practices for degraded grasslands. In 1992, the United Nations Agenda 21 listed desertification control, ecological monitoring of sensitive areas, and restoration of land degradation as core issues. Subsequent studies further confirmed that even severely damaged psammophytic meadows still have natural restoration potential. Under the guidance of the "Great Green Wall for the Sahara and the Sahel" initiative, Ethiopia and Nigeria have implemented large-scale ecological restoration on degraded land [2], which offers international references for ecosystem restoration and ecological-security improvement within agro-pastoral ecotones.

With the continuous development of ecosystem service assessment methods, remote sensing and geographic information technologies have provided important support for dynamic ecosystem monitoring. Domestic research teams have constructed a dynamic assessment framework for the service value of terrestrial ecosystems nationwide based on multi-source remote sensing information, including land-cover data from the First National Geographic Conditions Survey, MODIS enhanced vegetation index, and vegetation net primary productivity, laying a methodological foundation for regional ecosystem change and ecological security assessment.

However, for the agro-pastoral ecotone of Inner Mongolia, long-term quantitative identification of ecosystem type transitions and ecological security pattern evolution remains insufficient. Existing studies have not adequately characterized ecosystem structural changes and the evolution rate of ecological functions since 2000, and lack a systematic method for ecological security grading and assessment, making it difficult to accurately analyze the potential influencing mechanisms of climate change and human activities on ecological security.

Therefore, this study uses satellite remote sensing, land-cover, and meteorological observation data from 2000 to 2023, selects key indicators such as vegetation net primary productivity and normalized difference vegetation index [3], analyzes ecosystem transition conditions, and clarifies the spatial changes in ecological functions.

Different from many previous ecological security assessments that directly adopt the standard PSR framework without local adaptation, this study makes three targeted improvements for semi-arid agro-pastoral ecotone conditions. First, a PSR-entropy-weight indicator system coupling remote-sensing ecological variables and spatialized county-level socioeconomic statistics is constructed, considering the special human-land conflict characteristics of agro-pastoral zones. Second, to guarantee inter-annual comparability of long-term evaluation results, all ecological-security index values from 2000–2023 are pooled to generate unified classification thresholds, avoiding the defect of year-independent Jenks breaks that are widely used in existing literature. Third, besides describing static spatial patterns of ecological security, this work further explores statistical associations between ecological security and potential climatic and human-activity-related influencing factors.

https://doi.org/10.3390/su182110752

On this basis, an ecological security assessment system is constructed, so as to provide theoretical basis and practical support for strengthening the important ecological security barrier in northern China and supporting regional sustainable development.

2. Materials and Methods

2.1. Overview of the Study Area

Inner Mongolia Autonomous Region is the most important agricultural and pastoral production base in China. Owing to the long-term coexistence of agriculture and animal husbandry, combined with the region's unique natural geographical conditions, a long and narrow agro-pastoral ecotone has formed in Inner Mongolia, which is one of the eight major agro-pastoral ecotones in the world [4].

Due to differences in defining indicators, scholars from different disciplines have delineated different extents of the agro-pastoral ecotone. Based on definitions using climatic factors, meteorological indicators such as annual precipitation, annual mean temperature, and relative humidity are used to define the extent of the agro-pastoral ecotone [5,6]. This study adopts the boundary source of the agro-pastoral ecotone proposed by Professor An Pingli's team at China Agricultural University [7]. On this basis, several provinces and regions outside Inner Mongolia were removed, as were seven banners dominated by forest land in Hulunbuir City, such as New Barag Left Banner and Ewenki Autonomous Banner, and Siziwang Banner in Ulanqab City, which is dominated by grassland.

As shown in Figure 1, the agro-pastoral ecotone of Inner Mongolia has complex and diverse geomorphological types and severe terrain fragmentation. Elevation ranges from 87 to 2280 m, generally increasing from northeast to southwest. The northernmost part is the Hulunbuir Plateau, with an elevation of 650–750 m. Southward to the Horqin Sandy Land, the region forms a transition zone between the Northeast Plain and the Inner Mongolia Plateau, with an elevation of 200–700 m. Westward to the Bashang area of Hebei, it is located at the southern end of the Inner Mongolia Plateau, with an elevation of 1300–1800 m. The western Mu Us Sandy Land is located on the Ordos Plateau, with an elevation ranging from 1400 to 1500 m.

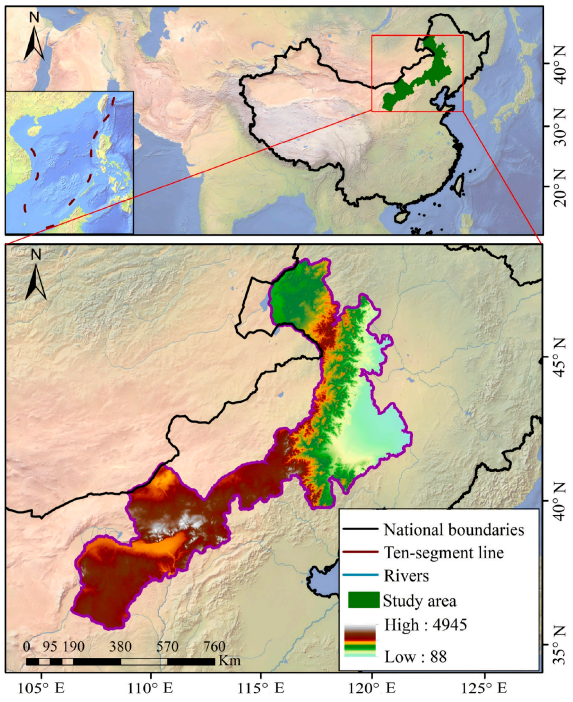


Figure 1. Overview of the study area of the agro-pastoral ecotone of Inner Mongolia.

2.2. Data Sources and Research Methods

This study adopted multi-source datasets with different temporal ranges. NDVI data were available for 2000–2023, and land-cover data spanned 1990–2023 [8]. Although the raw temperature and precipitation meteorological dataset covers 1980–2023, our actual analytical period is restricted to 2000–2023 due to the temporal availability limitation of MODIS NDVI products.

The land-cover dataset adopted in this work is the China Land-Use/Cover Change Dataset (CLUD). It has a spatial resolution of 1 km, with overall classification accuracy above 85% for agro-pastoral zones. The time-series product covers the years 1990, 2000, 2005, 2010, 2015, 2020 and 2023. Pre-processing steps included mosaicking, study-area clipping, reprojection to the WGS-84 coordinate system, and re-classification to aggregate original sub-classes into the six major ecosystem types used in this study: forest, grassland, cropland, desert, water-wetland, and settlement.

Precipitation and air-temperature records, sourced from the China Meteorological Administration, have an original time span of 1980–2023 and were interpolated into 1 km × 1 km raster grids combined with DEM data. Only the 2000–2023 subset of these meteorological rasters was used for all subsequent analyses matching NDVI and NPP time-series. NDVI was obtained from the NDVI raster product of the Moderate Resolution Imaging Spectroradiometer sensors of the National Aeronautics and Space Administration, with a 16-day temporal resolution and a 1 km × 1 km spatial resolution.

Data on cultivated land area, afforestation area, agricultural output value, animal husbandry output value, and output values of other industries were all obtained from statistical yearbooks.

The specific research methods are as follows:

The ecological pattern transition matrix is a two-dimensional matrix based on the change relationships of land-cover status in the same region at different time phases. It can reflect the area data of each land-cover type in a fixed region during a fixed period, as well as the area transferred out from each land-cover type in the initial stage and the area transferred into each land-cover type in the final stage (ArcGIS 10.8; Esri, Redlands, CA, USA).

Vegetation coverage model.

Vegetation coverage under the combined influence of climate and human activities was obtained from the MODIS data product NDVI [9]. First, the annual maximum NDVI was extracted from a series of NDVI values in the assessment year. Then, the vegetation coverage of each grid cell was calculated according to the following formula [10,11].

$$C_V = (V_{NDVI} - V_{NDVI-soil})/(V_{NDVI-MAX} - V_{NDVI-soil}) \quad (1)$$

In Equation (1), Cv is the vegetation coverage; V_{NDVI} is the annual-maximum normalized difference vegetation index. $V_{NDVI—soil}$ and $V_{NDVI—MAX}$ were derived from the statistical percentiles of annual-maximum NDVI pixels within the study area for each year. Specifically, $V_{NDVI—soil}$ corresponds to the 5th percentile of NDVI values, representing bare-soil signals; $V_{NDVI—MAX}$ corresponds to the 95th percentile of NDVI values, representing fully vegetated pixels. This percentile-based approach accounts for inter-annual variation in atmospheric and surface conditions across the study region.

Vegetation NPP model.

First, the maximum annual NDVI was extracted from 16-day MODIS NDVI time-series products. The study area contains multiple ecosystem types including forest, grassland, cropland, and desert-vegetation. A unified empirical-statistical framework (Equation (2)) was adopted for all land-cover pixels to simulate vegetation NPP, with elevation, annual

maximum NDVI, annual precipitation, and annual mean temperature as consistent input variables [12,13]. Given physiological differences across plant communities, minor disparities in simulation performance can be anticipated across land-cover categories for empirical-statistical models.

$$V_{NPP} = 6.353946 - 0.05875t + 0.003497p + 0.000275tp - 0.00065A + 1.793308V_{NDVI} \quad (2)$$

In Equation (2), NPP is the net primary productivity, t is the annual mean temperature, p is the annual precipitation, A is the elevation, and NDVI is the maximum normalized difference vegetation index within a year.

For NPP result validation, our simulated NPP outputs were qualitatively compared against published MOD17A2H NPP product and field-measured above-ground biomass sampling records from existing literature across Inner Mongolia agro-pastoral zones. Our simulated NPP exhibited broadly consistent spatial gradient patterns with reference datasets. Local magnitude deviations existed in extremely arid desert zones, which is a common limitation of empirical-statistical NPP models in arid-semiarid regions. It should be noted that this validation is purely qualitative. Due to the scarcity of spatially matched in situ biomass observations covering the full study domain, quantitative validation metrics are not provided in this work. Uncertainties originating from NPP simulation should be borne in mind when interpreting subsequent ecological-security index outputs and vegetation-climate correlation results.

It should be highlighted that annual mean temperature and annual precipitation serve as direct explanatory inputs within this empirical-statistical NPP model (Equation (2)). Consequently, correlation coefficients calculated between model-simulated NPP outputs and these two climate variables are partially constrained by the model's mathematical structure and do not represent fully independent empirical evidence for climatic attribution. Therefore, we mainly rely on the independently retrieved NDVI time-series for analyzing vegetation-climate associations in subsequent driver analysis, while the simulated NPP dataset is retained for ecological-security index calculation.

Construction of the ecological security risk assessment indicator system using the entropy weight method and PSR model.

Based on the comprehensive evaluation method, an ecological security risk assessment system was constructed. According to the driving factors of the spatiotemporal evolution of the ecological security pattern, the "pressure–state–response" (PSR) model was used to construct the ecological security risk assessment system. The three components of pressure, state, and response restrict and influence one another. Pressure indicators are used to reflect the causes and potential impacts of ecological environmental problems; state indicators are used to reflect changes in natural environmental conditions caused by human activities; and response indicators are used to reflect the capacity and responses of humans to overcome ecological environmental problems [14]. Indicators within the Pressure–State–Response framework were selected based on published ecological security studies for agro-pastoral ecotones, considering local human-environment interactions in the study area. Pressure indicators represent anthropogenic disturbance; state indicators reflect ecosystem natural background terrain and biophysical conditions, while response indicators denote human adaptive capacity and socioeconomic capacity for ecological management.

All indicator datasets were unified to a 1 km × 1 km grid spatial unit for subsequent processing, normalization, weight calculation and ecological-security index aggregation (R version 4.3.1; R Core Team, Vienna, Austria). All grid cells across the full study period (2000–2023) were pooled together to derive normalization thresholds and entropy weights to guarantee consistent inter-annual comparison.

Note that several socioeconomic indicators (total GDP, fertilizer application, agricultural machinery power, educational metrics, per capita-derived metrics, and irrigated area) are originally aggregated at the county-level administrative unit from statistical yearbooks. To match the 1 km × 1 km grid framework of the dataset, county-scale socioeconomic data were processed by two different spatial-processing strategies for absolute total-quantity variables versus rate/per capita/proportion variables.

For additive total-quantity variables (including total GDP, fertilizer application volume, total agricultural-livestock machinery power, and effective irrigated area), county-level total values were proportionally disaggregated into 1 km grid cells weighted by cropland fraction within each county grid.

For rate, percentage and per capita variables (including per capita GDP, percentage of population with high-school education or above, tertiary-industry proportion, science and technology level, and per capita urban green area), county-level original statistical values represent unit-based ratios or proportions that cannot be directly spatially split as additive totals. In this study, these county-scale ratio-type values were assigned to grids masked by built-up land within each county, assuming homogeneous socioeconomic conditions across built-up areas inside one county. It should be clarified that the "GDP" used in total-quantity spatial disaggregation refers to county-level total GDP, while Table 1 adopts the derived per capita GDP indicator for ecological-security assessment.

Table 1. Ecological security assessment indicator system.

Criterion Layer	Indicator Layer	Entropy Weight	Indicator Type for Ecological Security
Pressure (P)	Population density (people per square kilometer)	0.0612	−
	Fertilizer application volume (tons)	0.0647	−
	Total power of agricultural and livestock machinery (megawatts)	0.0582	−
	Proportion of cultivated land to total land area (%)	0.0705	−
Status (S)	Annual water output (mm)	0.0942	+
	Soil organic carbon content (g/m^2)	0.0786	+
	Net primary productivity of vegetation (g C/m′/a)	0.1084	+
	Vegetation coverage	0.1017	+
	PM2.5 concentration (micrograms/cubic meter)	0.0538	−
	Topographic undulation	0.0450	−
Response (R)	Luminous intensity	0.0472	−
	Habitat quality	0.0763	+
	Soil retention (t/ha)	0.0685	+
	Percentage of population with high school education or above (%)	0.0361	+
	Average green area per person in cities (square kilometers)	0.0314	+
	Proportion of the tertiary industry (%)	0.0337	+
	Per capita GDP (yuan per person)	0.0513	+
	Science and technology level (%)	0.0286	+
	Effective irrigated area (square kilometers)	0.0408	+

Note: This table presents the Pressure–State–Response (PSR) ecological-security evaluation indicator system. Entropy-weight values in the table are calculated by the entropy-weight method. The column "Indicator type for ecological security" denotes indicator attributes: "+" = positive indicator (higher value benefits ecological security); "−" = negative indicator (higher value impairs ecological security). All raster datasets were unified to a 1 km spatial resolution. County-level socioeconomic statistical data were spatially disaggregated into 1 km grids using auxiliary land-use datasets.

After spatial assignment, all gridded socioeconomic layers were resampled and unified to the consistent 1 km × 1 km resolution for subsequent standardization and index calculation. We acknowledge that this county-homogeneity assumption for ratio-type socioeconomic variables brings unavoidable spatial uncertainty; this limitation is further noted in the Discussion Section 4.

Positive and negative impact indicators were classified according to their different properties and standardized.

$$x'_{ij} = \frac{x_{ij} - min\{x_{ij}, \ldots\ldots, x_{nj}\}}{max\{x_{1j}, \ldots\ldots, x_{nj}\} - min\{x_{1j}, \ldots\ldots, x_{nj}\}} \tag{3}$$

$$x'_{ij} = \frac{max\{x_{ij}, \ldots\ldots, x_{nj}\} - x_{ij}}{max\{x_{1j}, \ldots\ldots, x_{nj}\} - min\{x_{1j}, \ldots\ldots, x_{nj}\}} \tag{4}$$

In Equations (3) and (4), n regions and m indicators are selected; thus, the value of the j-th indicator in the i-th region is obtained (i = 1, 2, . . ., n; j = 1, 2, . . ., m). Equation (3) corresponds to positive indicators, for which higher values contribute to higher ecological security. Equation (4) is applied for negative indicators, where higher raw values indicate greater ecological pressure. The maximum and minimum values of each indicator are calculated across the full study period.

The entropy method was used to calculate the weight of each indicator, so as to avoid excessive subjectivity in indicator selection and weight determination. The entropy weights for all indicators are reported in Table 1. These weights remain constant for the entire study period and are not recalculated for individual years.

The entropy-weight method was used to calculate the weight of each indicator, so as to avoid excessive subjectivity in indicator selection and weight determination. The full calculation workflow is presented step-by-step below.

First, calculate the indicator probability p_{ij} for normalized indicator values x'_{ij}:

$$p_{ij} = \frac{x'_{ij}}{\sum_{i=1}^{n} x'_{ij}} \tag{5}$$

where n is the total number of samples. Second, compute the entropy value e_j for indicator j:

$$e_j = -k\sum_{i=1}^{n}(p_{ij} ln p_{ij}) \tag{6}$$

where $k = 1/\ln(n)$, and $k > 0$. To avoid mathematical error caused by zero probability, we define $p^{ij} ln p_{ij} = 0$ when $p_{ij} = 0$.

Third, obtain the information utility value dj of indicator j:

$$d_j = 1 - e_j \tag{7}$$

A larger dj indicates that this indicator provides more effective evaluation information.

Finally, calculate the entropy-weight ω_j for each indicator j:

$$\omega_j = \frac{d_j}{\sum_{j=1}^{m} d_j} \tag{8}$$

where m is the total number of evaluation indicators. The entropy weights for all indicators are reported in Table 1. These weights remain constant for the entire study period and are not recalculated for individual years.

The comprehensive ecological security index (ESI) was obtained by weighted summation of all standardized indicators:

$$\mathrm{ESI} = \sum_{j=1}^{m} \omega_j x'_{ij} \quad (9)$$

In Equation (9), ω_j represents the entropy weight of indicator j, and x'_{ij} is the normalized value of indicator j.

For ecological-security level classification, the Jenks natural-breaks algorithm was adopted. Rather than computing separate Jenks breaks for each single year—which would produce variable class boundaries and undermine reliable temporal comparison of security grades—all ESI grid values across the whole study period (2000–2023) were pooled as one aggregated dataset to run the Jenks-optimized classification only once. The fixed classification boundaries presented in Table 2 are the direct output derived from this single global-sample Jenks calculation. These identical boundaries were consistently applied to re-classify ESI grids for every year in this study. This global-pooled-sample strategy prevents temporal-comparison bias caused by year-specific classification thresholds.

Table 2. Classification of ecological security levels in the agro-pastoral ecotone of Inner Mongolia.

Security Level	Safety Index	Level Characteristics
Unsafe	[0, 0.4)	The structure of the ecosystem is extremely unreasonable, the ecosystem services have severely deteriorated, the ability to resist interference is extremely poor, and the difficulty of ecological restoration is very high.
Less secure	[0.4, 0.45)	The structure of the ecosystem is highly unreasonable. The ecosystem has deteriorated, with a poor ability to resist interference and great difficulty in ecological restoration.
Critical security	[0.45, 0.5)	The degree of unreasonable structure of the ecosystem is relatively low. Although the ecosystem services have been damaged to some extent, they can still maintain basic operation and resist some disturbances. However, the restoration of the ecosystem is rather difficult.
More secure	[0.5, 0.55)	The ecosystem structure is relatively reasonable, and the ecosystem services have not undergone significant degradation. It has strong capabilities for recovery and resistance to interference.
Safety	[0.55, 1]	The ecosystem structure is reasonable, the ecosystem services have not deteriorated, it has strong anti-interference ability, and no ecological restoration or reconstruction is required.

Note: The five fixed classification thresholds for ecological-security levels in this table are derived from the Jenks natural-breaks algorithm. All grid-cell ecological-security index values across the entire study period (2000–2023) were pooled into one global aggregated dataset to compute breakpoints. These unified fixed thresholds are applied identically for every study year, which guarantees valid temporal comparison of ecological-security grades and avoids bias caused by year-specific separate Jenks classification.

3. Results

3.1. Hydroclimatic Characteristics and Ecological Transition

The agro-pastoral ecotone of Inner Mongolia is located in the transition zone between the eastern monsoon region of China and the northwestern continental climate region, and its climate type belongs to the temperate continental monsoon climate. The annual mean precipitation is approximately 134–636 mm and decreases from southeast to northwest. The northwestern part belongs to the continental arid monsoon region, with annual precipitation of less than 140 mm, where deserts and Gobi landscapes are widespread and

vegetation is sparse. The southeastern part belongs to the East Asian monsoon climate region, with relatively abundant precipitation and a relatively humid climate. The special geographical location leads to an unstable climate system [15]. Influenced by the tail end of the East Asian monsoon, changes in the strength of the southeastern monsoon and its north–south oscillation directly control the cold–warm and dry–wet climatic changes in this region (Figure 2).

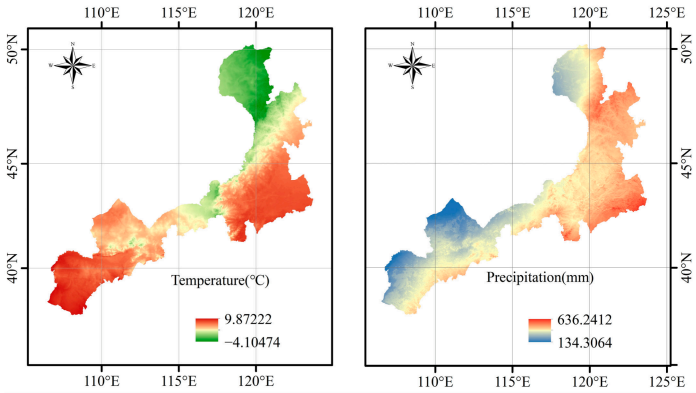


Figure 2. Spatial distribution of multi-year average temperature and precipitation in the agro-pastoral ecotone of Inner Mongolia.

During the period from 1990 to 2023, the ecosystem transitions in the agro-pastoral ecotone of Inner Mongolia are shown in Figure 3. The area of farmland ecosystems showed a decreasing trend and was mainly converted into grassland ecosystems, forest ecosystems, and settlement ecosystems. The area of forest ecosystems showed an increasing trend, and the increased area mainly came from grassland ecosystems and farmland ecosystems. The area of grassland ecosystems increased, mainly from farmland ecosystems and desert ecosystems. The areas of water body and wetland ecosystems decreased significantly and were mainly converted into farmland ecosystems, grassland ecosystems, and settlement ecosystems. The area of settlement ecosystems showed a sharp increasing trend, mainly from farmland ecosystems, grassland ecosystems, water body [16,17], wetland ecosystems, and desert ecosystems. The area of desert ecosystems showed a significant decreasing trend and was mainly converted into grassland ecosystems, farmland ecosystems, and settlement ecosystems.

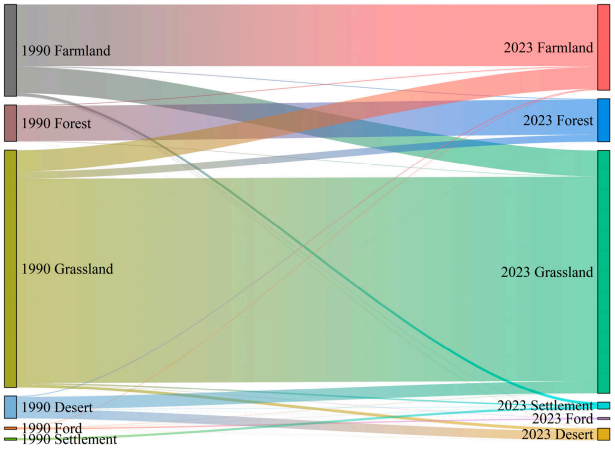


Figure 3. Overall ecosystem transition in the agro-pastoral ecotone of Inner Mongolia from 1990 to 2023.

3.2. Evolution Patterns of Ecological Quality and Functions

Based on remote sensing information and ground meteorological observation data, the normalized difference vegetation index and basic ecological functions of vegetation NPP in the agro-pastoral ecotone of Inner Mongolia were quantified at a spatial resolution of 1 km × 1 km. As shown in Figure 4, from 2000 to 2023, the average NPP of the agro-pastoral ecotone of Inner Mongolia was 657.7 g/m^2/a, and the NDVI was 0.51. Ecological functions showed significant spatial differences and similar spatial distribution patterns. From 2000 to 2023, both NPP and NDVI in the agro-pastoral ecotone of Inner Mongolia showed an increasing distribution trend from northwest to southeast [18,19]. Among them, the lowest NPP value appeared in the northwestern part of the study area, approximately 499.78 g/m^2/a, while the highest value appeared in the northeastern part, approximately 778.49 g/m^2/a. The general pattern of NPP change also increased from southwest to northeast. Different from the total value, the area with the slowest change in NPP appeared in the central-western junction area of the agro-pastoral ecotone [20], while the maximum change amplitude appeared in the eastern region. Overall, both the total value and the change value of NPP show relatively obvious spatial differences, and generally increase from northwest to southeast [21].

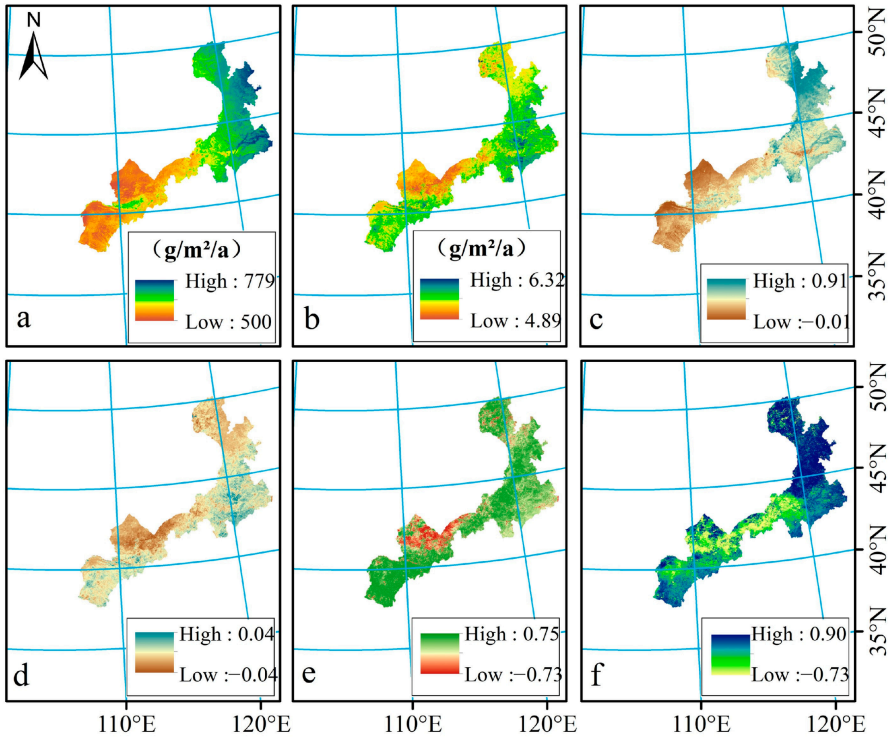


Figure 4. Distribution map of ecological function changes from 2000 to 2023. Note: (**a**) Spatial distribution of total NPP; (**b**) Spatial distribution of NPP changes; (**c**) Spatial distribution of NDVI; (**d**) Spatial distribution of NDVI changes; (**e**) Spatial pattern of correlation coefficients between temperature and NDVI; (**f**) Spatial pattern of correlation coefficients between precipitation and NDVI.

The overall distribution of NDVI values was similar to that of NPP, but the spatial differences in NDVI changes across the entire study area were relatively small, with more than 50% of the region showing small changes or negative growth. Existing studies have shown that the effects of temperature and precipitation on NDVI have a spatial trade-off relationship. This study analyzed the relationship between NDVI and temperature and precipitation in the agro-pastoral ecotone of Inner Mongolia from 2000 to 2023. The results showed that in a small part of the western region, the correlation between NDVI and temperature reached −0.72, while the highest correlation between NDVI and precipitation

exceeded 90%, occurring in the northwestern region. The correlation between precipitation and NDVI was higher than that between temperature and NDVI [22], and increases in both temperature and precipitation were correlated with increased plant growth. Overall, the vegetation NPP capacity of the agro-pastoral ecotone of Inner Mongolia improved significantly, directly reflecting the improvement of vegetation ecological quality and ecological function [23], and indicating that the combined effects of climate change and human activities are associated with the positive development of the regional ecosystem [24].

Theoretically, both air temperature and precipitation are closely related to vegetation ecological quality, and changes in air temperature and precipitation are important potential influencing factors of vegetation change [24,25]. Since the average temperature of the agro-pastoral ecotone of Inner Mongolia is relatively low, low temperature is one of the important factors limiting plant growth. Rising temperature helps to prolong the vegetation growing season and improve vegetation coverage and net primary productivity. The agro-pastoral ecotone of Inner Mongolia is generally relatively arid, and increased precipitation provides more sufficient water for vegetation [26].

Linear trend analysis was performed for annual mean temperature, annual total precipitation, area-averaged NPP and NDVI over 2000–2023. For annual mean temperature, the trend slope was 0.02558 $^{\circ}C \cdot yr^{-1}$ ($p > 0.05$), showing an apparent but statistically non-significant warming tendency. Annual total precipitation exhibited a significant upward trend with slope of 0.39504 $mm \cdot yr^{-1}$ ($p < 0.05$). Area-averaged NPP increased markedly, with a slope of 10.05312 $g\ C \cdot m^{-2} \cdot yr^{-1}$ ($p < 0.001$). The NDVI also presented a significant increasing trend, with slope equal to 0.0044 yr^{-1} ($p < 0.001$).

Pearson correlation was applied to explore pairwise relationships between climate variables and vegetation indicators. Temperature showed weak positive correlations with NPP (r = 0.234) and NDVI (r = 0.141). Precipitation was positively correlated with NPP (r = 0.688) and NDVI (r = 0.823). It should be noted that time-series data may be affected by temporal autocorrelation and shared common trends, which potentially inflate correlation significance. Accordingly, these coefficients only reflect statistical association rather than definite causal relationships between climate and vegetation.

As shown in Figure 5, the agro-pastoral ecotone of Inner Mongolia exhibited an apparent warming tendency together with a statistically significant wetting trend from 2000 to 2023, which coincided with the improvement of vegetation production functions. To explore statistical associations between climatic warming-wetting conditions and ecological functions in the agro-pastoral ecotone of Inner Mongolia, we analyzed interannual variation trends of ecological-function indicators and climatic indicators (precipitation and air temperature) during 2000–2023. The results showed that NDVI had a low correlation with temperature (r = 0.14), but a high correlation with precipitation (r = 0.82). The results indicate that precipitation exhibits a comparatively stronger statistical association with NDVI relative to temperature in the agro-pastoral ecotone. Since precipitation and temperature are built-in inputs of our empirical-statistical NPP model, the correlation between simulated NPP and precipitation (r = 0.688) cannot be treated as independent evidence of climatic driving. We report this coefficient for reference only. The minimum values of annual precipitation and net primary productivity both occurred in 2007. In addition, vegetation net primary productivity and annual precipitation also showed relatively consistent upward and downward trends.

At the multi-year timescale, both annual mean temperature and annual precipitation showed positive statistical associations with vegetation ecological functions, yet the correlation coefficients for temperature were very low (r = 0.14–0.23). While moderate warming may be beneficial under sufficient moisture conditions, interannual time-series fluctuations imply that high temperature can impose potential stress on vegetation during

years with low precipitation. Vegetation function valley values occasionally coincided with temperature peaks, whereas vegetation peaks consistently matched high-precipitation years. This further indicates that precipitation shows stronger statistical association with vegetation conditions, while the statistical linkage between long-term moderate warming and vegetation is weak across this semi-arid ecotone.

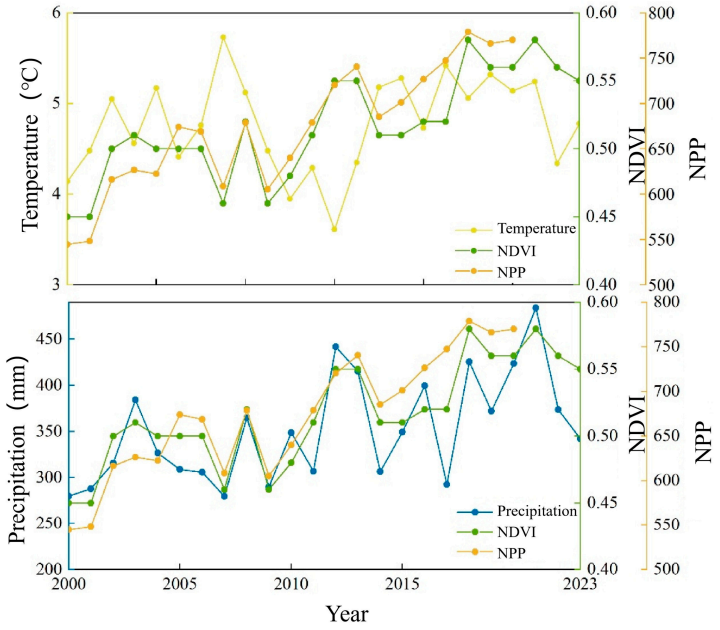


Figure 5. Inter-annual time-series variations in temperature, precipitation, NDVI and NPP across the study area during 2000–2023.

3.3. Construction of the Risk Assessment System and Spatiotemporal Distribution Transition

As shown in Table 1, combined with the driving factors of ecological security pattern evolution in the basin, this study constructed an ecological security risk assessment system using the comprehensive evaluation method and the PSR model, and characterized the causes of ecological environmental problems, changes in the natural environment, and human response measures from the three aspects of pressure, state, and response [27].

1. Population density: source: statistical yearbooks; spatialized to 1 km grid; time series: 2000–2023; negative indicator. 2. Per capita GDP: source: statistical yearbooks; spatialized to 1 km grid; time series: 2000–2023; positive indicator. 3. Fertilizer application volume: source: statistical yearbooks; spatialized to 1 km grid; time series: 2000–2023; negative indicator. 4. Total power of agricultural-livestock machinery: source: statistical yearbooks; spatialized to 1 km grid; time series: 2000–2023; negative indicator. 5. Proportion of cultivated land: source: CLUD land-cover dataset, 1 km; time series: 2000–2023; negative indicator. 6. Annual water output: source: hydrological dataset, 1 km; time series: 2000–2023; positive indicator. 7. Soil organic carbon content: source: soil dataset, 1 km; static spatially constant layer; positive indicator. 8. Net primary productivity of vegetation: source: empirical-statistical simulation output driven by MODIS NDVI and meteorological data, 1 km; temporal coverage: 2000–2023; positive indicator. 9. Vegetation coverage: source: MODIS-NDVI derived, 1 km; time series: 2000–2023; positive indicator. 10. PM2.5 concentration: source: atmospheric remote-sensing product,1 km; time series: 2000–2023; negative indicator. 11. Luminous intensity: source: night-time light remote-sensing product, 1 km; time series:2000–2023; negative indicator. 12. Habitat quality: source: InVEST model output,1 km; time series:2000–2023; positive indicator. 13. Soil retention: source: RUSLE model output,1 km; time series: 2000–2023; positive indicator. 14. Topographic un-

dulation: source: DEM, 1 km; static layer; negative indicator. 15. Percentage of population with high-school education and above: source: statistical yearbooks; spatialized to 1 km grid; time series: 2000–2023; positive indicator. 16. Per capita urban green area: source: statistical yearbooks; spatialized to 1 km grid; time series: 2000–2023; positive indicator. 17. Tertiary-industry proportion: source: statistical yearbooks; spatialized to 1 km grid; time series:2000–2023; positive indicator. 18. Science-technology level: source: statistical yearbooks; spatialized to 1 km grid; time series: 2000–2023; positive indicator. 19. Effective irrigated area: source: statistical yearbooks; spatialized to 1 km grid; time series:2000–2023; positive indicator.

The comprehensive index method is a widely used method in ecological security evaluation. It calculates the comprehensive ecological security index through weighted summation [28]. A higher index value indicates higher ecological security, while a lower value indicates greater vulnerability. Common classification methods include the equal-interval method, expert method, and natural breaks method, among which the equal-interval method is commonly adopted. However, this study found that the traditional method for calculating security levels could not effectively reflect the internal differences within the agro-pastoral ecotone of Inner Mongolia. Therefore, the natural breaks method was used to reclassify the ecological security index. By reducing intra-class differences and maximizing inter-class differences, the natural breaks method better reflects the internal differences in ecological security within the agro-pastoral ecotone of Inner Mongolia.

The ecological index and state subsystem of the agro-pastoral ecotone of Inner Mongolia generally showed an upward trend, while the response subsystem showed a continuous downward trend after a brief increase, and the overall change trend of the pressure subsystem was relatively stable (Figure 6). The decline of the response subsystem since 2005 may be associated with multiple factors. Ecological-pattern shifts within the agro-pastoral ecotone of Inner Mongolia may exert influences on ecological security. Ecological-pattern alterations linked to overgrazing and unreasonable agricultural cultivation are suspected to correlate with declining ecosystem-service functions, which may further affect the stability and effectiveness of the response subsystem. Ecological degradation may have weakened the ability of ecosystems to respond to external disturbances. Such degradation reduces ecosystem resilience, making it more difficult for the system to recover from disturbances.

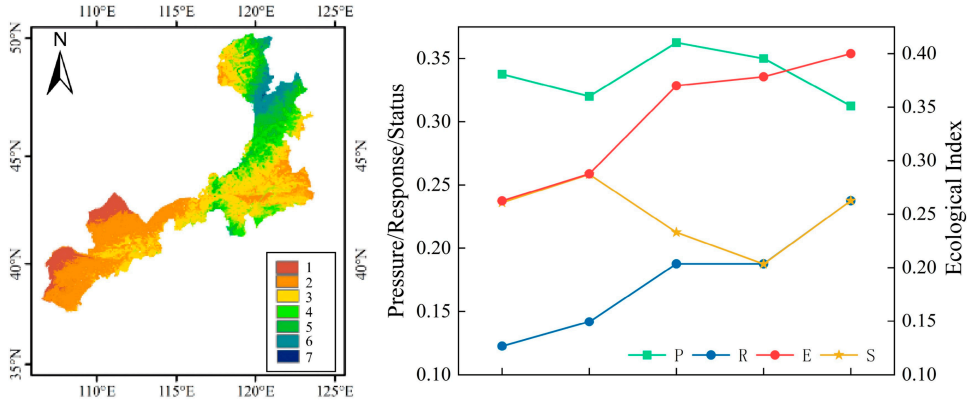


Figure 6. Analysis of ecological health change trends in the study area. **Note:** 1–7 represent significant improvement, relatively significant improvement, slight improvement, stable improvement, slight deterioration, relatively significant deterioration, and significant deterioration.

The continuous upward trend of the state subsystem is related to major ecological protection and restoration projects, such as the grassland ecological protection subsidy and reward policy, grazing prohibition and grassland restoration, and conversion of farmland to grassland, as well as changes in vegetation coverage and ecological restoration.

The classification of ecological security levels in the agro-pastoral ecotone of Inner Mongolia is shown in Table 2. Combined with Figure 7, the northeastern region is mainly composed of "relatively secure" and "secure" areas, with a reasonable ecosystem structure and strong anti-disturbance capacity, whereas the southwestern region is mainly composed of "insecure" and "relatively insecure" areas, with an unreasonable ecosystem structure and severe degradation. The central region between the north and south is mostly distributed with the "critical security" level. Although the ecosystems in these areas have been damaged to some extent, they maintain basic operation and have a certain recovery capacity, serving as an important transitional zone between the northern and southern ecological security levels.

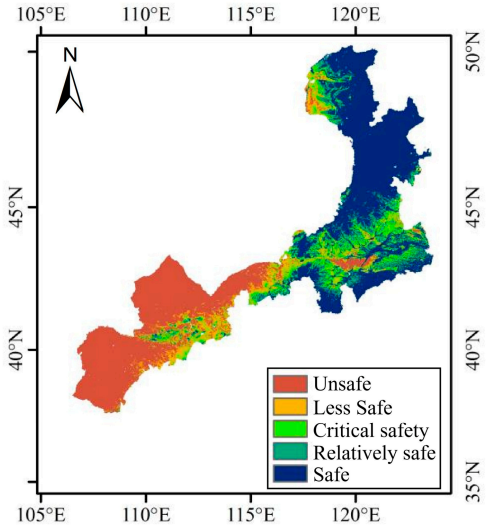


Figure 7. Distribution of ecological security levels in the study area.

The ecological security status of the agro-pastoral ecotone of Inner Mongolia showed a pattern of overall improvement and local decline. Insecure areas accounted for more than 50%, mainly concentrated in Ulanqab City and areas to its west, including Baotou City, Hohhot City, and Ordos City. The northeastern areas, including Hulunbuir City, Chifeng City, Hinggan League, and Tongliao City, mainly showed relatively secure and secure trends. The ecological security status in the northeastern region was relatively good and showed an improving trend, indicating relatively high recovery capacity and stability. In contrast, the ecological security status in the southwestern region was relatively poor, with a significant degradation trend, and the ecosystem faced greater threats. The pressure on the ecosystem continued to increase, but the response capacity and state gradually improved, indicating that the ecological security status of local ecosystems tended to stabilize to some extent.

From 2000 to 2023, the ecological security levels of the agro-pastoral ecotone of Inner Mongolia showed obvious changes (Figure 8). Over the past two decades, areas with relatively high ecological security levels in the agro-pastoral ecotone of Inner Mongolia were relatively limited, mainly concentrated in the Greater Khingan Mountains and Hulunbuir Grassland in the northeast. From 2000 to 2015, in some years, ecologically relatively insecure and insecure areas exceeded 50%, and these areas were concentrated in the central and southwestern regions. Compared with 2000, the ecologically insecure areas decreased in 2010, but the relatively insecure areas increased by 1.02 times. By 2015 and 2020, although ecological security had improved, desertification and grassland degradation in the western region remained relatively severe and still showed low ecological security levels, indicating that recovery in the eastern and central regions was relatively good, while the western

region faced greater restoration pressure. After 2020, the overall ecological security level improved, and some relatively insecure areas shifted to critical security or relatively secure levels; however, the economically developed areas in the southwest still faced ecological security problems.

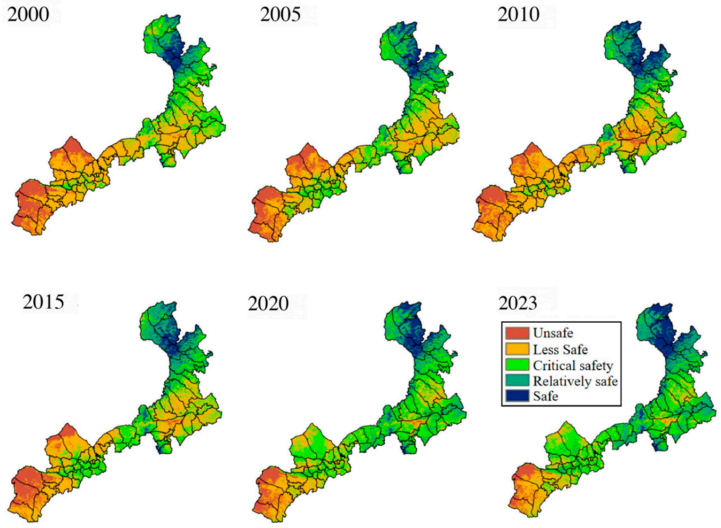


Figure 8. Spatiotemporal distribution of ecological security in the study area from 2000 to 2023.

The spatiotemporal transition of ecological security evaluation levels in the study area from 2000 to 2023 was analyzed, and the areas and area sizes where ecological security evaluation levels remained unchanged, increased, or decreased between adjacent years were obtained. The results are shown in Figure 9. According to Table 3, from 2000 to 2005, the area with increased ecological security was 16.09 $\times$ 10^4 km^2, mainly concentrated in the southwestern part of the ecotone, parts of the central region, and parts of the northeastern region. The area with decreased ecological security was 7.80 $\times$ 10^4 km^2, concentrated in the eastern part of the ecotone. From 2005 to 2010, the area with increased ecological security was 11.18 $\times$ 10^4 km^2, while the decrease was relatively large, approximately 14.00 $\times$ 10^4 km^2, mainly distributed in the eastern and western regions. From 2010 to 2015, the area with increased ecological security expanded significantly, mainly concentrated in the central and southwestern regions, while areas with decreased ecological security appeared in the northeastern region. From 2015 to 2023, the area with increased ecological security was the largest, reaching 30.54 $\times$ 10^4 km^2, mainly concentrated in the eastern and northwestern regions. Overall, from 2000 to 2023, the agro-pastoral ecotone of Inner Mongolia showed a steady upward trend, and areas that were originally stable gradually tended to improve.

The ecological security levels of the agro-pastoral ecotone of Inner Mongolia have shown substantial dynamic changes over the past more than 20 years. From 2000 to 2005, ecological security improved slowly, and areas with degraded ecological security were relatively extensive. From 2005 to 2010, although the magnitude of improvement increased, the northwestern region still faced considerable ecological pressure. From 2010 to 2015, ecological security improved significantly, especially in the eastern and central regions, whereas the western region still faced major restoration challenges. By 2015–2023, the overall ecological security had improved significantly, particularly associated with the restoration of grasslands and wetlands, and ecological security levels gradually increased. However, greater efforts are still needed in the western desertified areas.

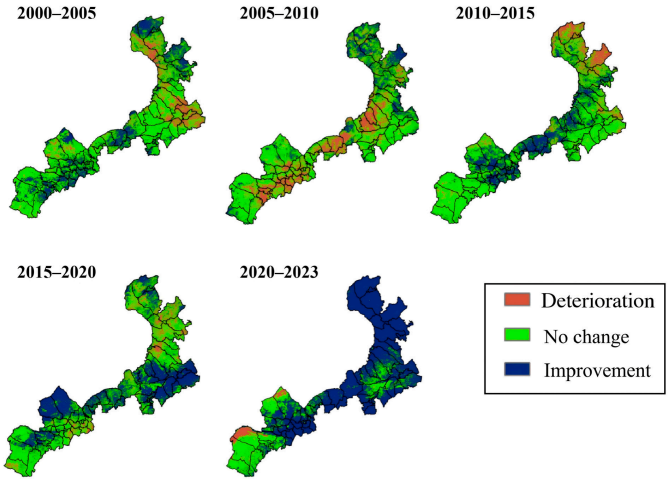


Figure 9. Distribution of ecological security transitions in the study area from 2000 to 2023.

Table 3. Changes in ecological security transition area in the study area from 2000 to 2023 (unit: 10^4 km^2).

Serial Number	Time Series	Improved Area	Deteriorated Area	Unchanged Area
1	2000–2005	16.09	7.80	43.83
2	2005–2010	11.18	14.00	42.54
3	2010–2015	21.25	4.93	41.55
4	2015–2023	30.54	2.63	34.55

Changes in ecological security levels are closely related to climate change and human activities. Although the study-area-averaged climate shows an overall warming-wetting trend, the arid south-western zones still suffer from high inter-annual precipitation variability and frequent extreme-drought episodes. Rising temperature amplifies evapotranspiration and exacerbates water-resource stress for desert-prone localities. Desertification and water-resource shortages in the west have seriously affected the ecological-security level of this region. Meanwhile, human activities such as overgrazing and land reclamation have intensified ecological degradation in these areas. On the other hand, ecological restoration measures such as grassland restoration and wetland protection have significantly improved the ecological environment in the eastern and central regions. Although ecological security has improved over the past more than 20 years, desertification and water-resource problems in the west remain the major challenges for the future. To address these problems, ecological restoration efforts should be strengthened, especially vegetation restoration and sand-fixation projects in desertified areas, while promoting the application of water-saving irrigation and green agricultural technologies. At the same time, policy support and supervision should be strengthened, and ecological compensation mechanisms and ecological reserves should be promoted to facilitate continuous improvement of the regional ecological environment and enhancement of ecological security [29,30].

4. Discussion

This study systematically analyzed the spatiotemporal characteristics of ecological pattern transition, ecological function evolution, and ecological security risks in the agro-pastoral ecotone of Inner Mongolia from 2000 to 2023. The results show that the regional ecological environment generally exhibited a positive development trend, with significant spatial differentiation and prominent local problems. The evolutionary process appears to be associated with combined effects of climate change and human activities, and thus

requires in-depth discussion from the perspectives of driving mechanisms, pattern characteristics, and key problems.

To verify the reliability of our ecological-security classification results, we compared the spatial pattern obtained in this study with previously published ecological-security assessment studies for the Inner Mongolia agro-pastoral ecotone, as well as publicly observed desertification and grassland-degradation monitoring records [31,32]. Generally, our spatial pattern is consistent with existing regional research: high ecological security is concentrated in the northeastern forest-grassland zone of the study area, while low-security areas are mainly distributed in the arid southwestern part, which corresponds to high desertification risk and grassland degradation records in this zone [31–34]. Nevertheless, several local spatial discrepancies can still be detected. For some transitional agro-pastoral zones, our ecological-security values are moderately higher compared with some earlier assessments, which may be attributed to the continuous ecological restoration effects from long-term ecological projects after 2000 [35,36]. Such cross-comparison supports the overall reliability of our ecological-security classification, while also implying that local transitional zones still exist uncertainties in assessment.

Comparing our results with ecological-security assessments from other northern dryland and agro-pastoral transition zones, similar spatial patterns can be observed: ecological security generally decreases from humid eastern parts toward arid western inland areas, and precipitation acts as a primary limiting factor for ecosystem status across most semi-arid agro-pastoral regions. Consistent with studies for the Loess Plateau and northern farming-pastoral ecotone, human-land conflicts concentrated in transitional zones constitute major threats to local ecological security [32,37]. Nevertheless, some differences also exist. Compared with adjacent arid regions, our study area shows a more obvious improvement trend after 2015, which may relate to the targeted implementation of grassland-oriented ecological restoration projects within Inner Mongolia [36]. These inter-regional comparisons further contextualize the spatial characteristics and changing tendency observed in our work.

From the perspective of climatic associations, the regional warming-wetting trend provided favorable hydrothermal background conditions for vegetation growth. Based on the independent NDVI observations, precipitation shows much stronger statistical association with vegetation status than temperature. Caution is required when interpreting correlation outputs from our model-simulated NPP, because temperature and precipitation are explicit predictors inside Equation (2); those NPP-climate correlations are partially imposed by model structure and are not used for our main climatic inference in this study. This is highly consistent with the generally arid climatic background of the agro-pastoral ecotone. The arid and low-precipitation characteristics of the northwestern region make vegetation growth more sensitive to water supply. Although rising temperature can prolong the vegetation growing season, under an arid background it may intensify soil evapotranspiration and instead exert potential adverse effects on local ecological functions. This observation suggests that precipitation represents a key correlated factor for vegetation ecological functions in semi-arid regions, and also helps to explain the spatial pattern of ecological functions increasing from northwest to southeast, which is consistent with general climate-vegetation correlation patterns reported for northern China's agro-pastoral ecotone.

It should be noted that the positive statistical association between hydro-thermal conditions and vegetation improvement does not directly confirm causal effects. For trending time-series data such as our long-term dataset, significant correlation coefficients may arise from shared temporal trends and do not necessarily represent genuine cause-and-effect links. The regional warming-wetting trend provides a favorable climatic background for

vegetation recovery, yet ecological improvement cannot be fully attributed to climatic variation alone. A series of large-scale ecological restoration policies were continuously implemented across the study domain over the same period, including grazing prohibition, grassland conservation and conversion of farmland to grassland. Climatic background and human-led restoration measures may produce synergistic effects on vegetation recovery. Given the limitation of current correlation-based analysis, we cannot quantitatively disentangle their respective independent contributions, which remains a key issue for follow-up research.

From the perspective of bidirectional human-activity effects, the implementation of ecological engineering projects may be associated with the observed increase in forest and grassland areas and improved ecological functions, as suggested by previous regional studies [31,34–36]. Policies including grassland ecological-protection subsidies, grazing prohibition, grassland restoration, and grain-for-forest programs may create potentially favorable background conditions for natural-ecosystem recovery, which may partly correspond to the sustained high ecological-security level across the northeastern forest-grassland zone. Nevertheless, unreasonable human-related disturbances may threaten regional ecological security. Rapid settlement expansion can occupy farmland, forest, grassland, water-body and wetland resources. Overgrazing and inappropriate agricultural practices have been hypothesized to weaken ecosystem self-recovery capacity and may correlate with the declining response-subsystem trend. Resource exploitation and intensive agricultural activities in the economically developed southwest may exacerbate land desertification and water scarcity, rendering this zone a persistent ecological-security hotspot of vulnerability [35,37]. It should be emphasized that such human-driven interpretations are inferred from existing literature; our current dataset cannot quantitatively disentangle the independent contribution of anthropogenic impacts.

From the perspective of the coupling relationship between ecological patterns and security, reasonable transitions of ecosystem types have a positive promoting effect on the improvement of ecological security. The increase in forest and grassland areas directly improved state indicators such as regional NPP and vegetation coverage, thereby increasing the ecological security index. In contrast, pattern changes such as desert expansion, water body shrinkage, and disorderly settlement growth intensified ecosystem vulnerability, leading to long-term low ecological security levels in the southwestern region. In addition, the spatiotemporal transition characteristics of ecological security show that after 2015, the improvement of ecological security in the study area increased significantly. This is closely related to China's recent increase in investment in ecological protection and restoration and the strategic deployment of integrated protection of mountains, rivers, forests, farmland, lakes, grasslands, and deserts, reflecting the important guiding role of policy intervention in optimizing the ecological security pattern.

Nevertheless, this study still has certain limitations. Although the indicator selection of the ecological security assessment system was based on the PSR model, indicators such as extreme climate events and biodiversity were not included, resulting in an incomplete characterization of ecological security. This study focused on the overall evolution characteristics of a long time series, while insufficient attention was paid to short-term fluctuations in ecological patterns and security and their driving factors. Future studies can combine contribution rate models to quantify the relative contributions of natural and human factors, improve the ecological security assessment indicator system, and strengthen research on the impacts of extreme climate on regional ecological security, thereby improving the accuracy and applicability of the results.

In addition, spatial gridding of county-scale per capita and proportion-based socioeconomic indicators relies on the within-county homogeneity assumption for built-up areas.

This approximate spatialization may introduce uncertainties for gridded indicator values and the resulting ecological-security index and spatial maps. Future work will explore more sophisticated disaggregation approaches for ratio-type socioeconomic variables.

In addition, although ecological security in the study area has generally improved, problems such as desertification in the west, water resource shortages, and conflicts between settlement expansion and ecological protection in the southwest remain urgent to resolve. According to our assessment results, high-security conditions are mainly distributed in the northeastern forest-grassland zone, low-security risks concentrate in the arid southwest, and the central zone represents a critical transitional status. Targeted restoration strategies should match such spatial-risk features derived from our ecological-security classification. Therefore, this study proposes differentiated ecological restoration strategies for different regions based on above-mentioned analytical outputs.

For regions with a good ecological background, such as the Hulunbuir Grassland, the forest transition zone of the Greater Khingan Mountains, and the wetlands of the Hetao Plain, which mainly include areas with rich biodiversity, important ecological functions, and high ecological vulnerability, the primary objective is to maintain the original state and integrity of existing ecosystems to the greatest extent, protect and restore ecosystem service functions, and maintain core ecological functions. Strict protection measures should be implemented to reduce disturbance from human activities and prohibit destructive activities such as overgrazing, illegal harvesting, and indiscriminate logging. By strengthening ecological monitoring and scientific assessment, changes in the ecological environment can be monitored in real time to ensure the long-term stability of ecosystems. For areas with severe degradation, such as grassland desertification and soil salinization, the restoration objective is to restore ecological functions and enhance ecosystem resilience and stability through comprehensive restoration measures. Ecological restoration areas should adopt systematic restoration measures, conduct soil remediation, improve soil quality, and prevent soil erosion and desertification. Through vegetation restoration projects, the ecological functions of grasslands and forests should be restored, vegetation coverage should be increased, and soil and water loss should be reduced. For areas where ecological protection and economic development can be coordinated, restoration and regulation strategies should promote green economic development. Ecological infrastructure should be constructed to improve ecosystem service capacity, optimize resource allocation, and promote the coordinated integration of the ecological environment with social and economic development. Regional coordinated development policies should be implemented to balance population growth, land use, and ecological protection, ensure sustainable development, and enhance ecological security.

In addition, the current analysis is mainly built on correlation statistics. Although we can observe associations between climatic-human factors and ecological-security variations, this study cannot quantitatively separate the independent contribution of climate change and human-activity interference. Further quantitative attribution approaches such as variance partitioning or structural equation modeling are required to disentangle their relative importance, which will be implemented in our future research.

5. Conclusions

This study systematically analyzed the spatiotemporal characteristics of ecological pattern transition, ecological function evolution, and ecological security risks in the agro-pastoral ecotone of Inner Mongolia from 2000 to 2023, and explored the joint potential influences of climate change and human activities. The ecosystem in the study area generally showed positive evolution, with increases in forest and grassland areas and a decrease in desert area, but the problems of water body and wetland shrinkage and settlement

expansion were prominent. The regional warming and wetting trend provided favorable conditions for ecological restoration. Based on independent NDVI observations, precipitation exhibited markedly higher correlative association with vegetation conditions than temperature. Correlations for model-simulated NPP against climate are partially constrained by model inputs and are not used for primary climatic inference. These patterns jointly produce the spatial gradient of ecological functions increasing from northwest to southeast. The ecological security status improved steadily overall, showing significant spatial differentiation characterized by "security in the northeast, insecurity in the southwest, and critical status in the central region". After 2015, the magnitude of ecological improvement increased markedly, and the area showing improvement continued to expand. Ecological projects such as grassland ecological protection, grazing prohibition and grassland restoration may serve as plausible contributing factors for the improvement of ecological functions and ecological security, while overgrazing, unreasonable agricultural cultivation, and disorderly settlement expansion are suspected to be associated with local ecological degradation, with the southwestern region maintaining particularly high ecological vulnerability. Such human-related influences cannot be quantitatively isolated in the present correlation-based analysis. Based on the above conclusions, differentiated ecological restoration strategies should be implemented in the future. Natural restoration should be prioritized in the northeast, desertification control and water resource security should be emphasized in the southwest, ecological buffer zone construction should be strengthened in the central region, and ecological protection policies and dynamic monitoring systems should be continuously improved, so as to promote the coordinated advancement of ecological protection and economic development and consolidate the ecological security barrier in northern China.

Author Contributions: Conceptualization, Z.Z., L.M. and B.S.; methodology, Z.Z.; software, B.S.; validation, Z.Z.; formal analysis, Z.Z.; investigation, Z.Z., J.Y., and C.W.; resources, L.M., Q.Z.; data curation, L.M. and B.S.; writing—original draft preparation, Z.Z.; writing—review and editing, Z.Z., L.M. and B.S.; visualization, X.H.; supervision, L.M. and B.S.; project administration, L.M. and B.S.; funding acquisition, L.M. and B.S. All authors have read and agreed to the published version of the manuscript.

Funding: This work was supported by the 2025 Key Laboratory of Eco-hydrology and Efficient Water Resources Utilization, Inner Mongolia Autonomous Region—Evolution and Driving Mechanism of Ecological Environment in the Wuliangsuhai Watershed (Grant No. 2025KYPT0091); Research Start-up Project for the Introduction of High-level and Outstanding Doctoral Talents at Inner Mongolia Agricultural University (Funder: Bolin Sun, Grant No. NDYB2023-28). The authors gratefully acknowledge all funding agencies for their scientific sponsorship.

Institutional Review Board Statement: Not applicable.

Informed Consent Statement: Not applicable.

Data Availability Statement: Publicly available datasets utilized in this study include the CLUD land-cover dataset, MODIS-NDVI product, MOD17A2H NPP product, and meteorological observation datasets from the China Meteorological Administration. All these open datasets can be accessed via their respective official public repositories. County-level socioeconomic statistical datasets are not hosted in public repositories and are not publicly accessible; these datasets may be obtained from the corresponding authors upon reasonable request.

Conflicts of Interest: The authors declare no conflicts of interest.

References

1. Zhu, L.; Zhu, W.L. Domestic and overseas review of land desertification control and ecological restoration. *J. Hum. Settl. West China* **2020**, *35*, 97–103.
2. Goffner, D.; Sinare, H.; Gordon, L.J. The Great Green Wall for the Sahara and the Sahel Initiative as an opportunity to enhance resilience in Sahelian landscapes and livelihoods. *Reg. Environ. Change* **2019**, *19*, 1417–1428. [CrossRef]
3. Cheng, T. A calculating and analyzing method of national land ecosystem service values big data. *Bull. Surv. Mapp.* **2018**, *8*, 41–46.
4. Chen, X.P.; Zhao, X.Y.; Wang, R.X.; Ning, Z.; Lu, J.; Zhao, S. Research advances on the impact of climate change and LUCC for water resources in the northern agro-pastoral zone in China. *J. Desert Res.* **2022**, *42*, 170–177.
5. Zhu, Z.D.; Liu, S. Desertification process and its control zoning in northern China. *J. Desert Res.* **1981**, *1*, 16.
6. Chen, Q.G.; Zhang, J.; Yang, L.N. Calculation and simulation of the agro-pastoral ecotone in China based on GIS. *J. Lanzhou Univ. Nat. Sci.* **2007**, *43*, 24–28.
7. Chen, X.; Jiang, L.; Zhang, G.L.; Meng, L.; Pan, Z.; Lun, F.; An, P. Green-depressing cropping system: A referential land use practice for follow to ensure a harmonious human-land relationship in the farming-pastoral ecotone of northern China. *Land Use Policy* **2021**, *100*, 104917. [CrossRef]
8. Jiang, W.G.; Chen, Y.H.; Li, J.; Li, J.; Wu, Y. Change and Spatial Pattern of Eco-environment in the Farming-pastoral Ecotone of the Northern China. *J. Nat. Resour.* **2005**, *20*, 871–878.
9. Chen, H.; Fleskens, L.; Schild, J.; Moolenaar, S.; Wang, F.; Ritsema, C. Impacts of large-scale landscape restoration on spatio-temporal dynamics of ecosystem services in the Chinese Loess Plateau. *Landsc. Ecol.* **2022**, *37*, 329–346. [CrossRef]
10. Liu, C.; Liu, B.; Zhao, W.Z.; Zhu, Z.; Si, R. Temporal-spatial variation analysis of net primary productivity and its relationship with climate in central Asia. *Remote Sens. Technol. Appl.* **2020**, *35*, 924–933.
11. Li, M.; Wang, C.; Zhang, X. Identification of the candidate areas of ecological protection red lines based on water conservation function in territory spatial planning. *Geogr. Res.* **2019**, *38*, 2447–2457.
12. Yuan, Y.; Bao, A.M.; Liu, T.; Zheng, G.X.; Jiang, L.L.; Guo, H.; Jiang, P.; Yu, T.; De Maeyer, P. Elevation Gradients Limit the Antiphase Trend in Vegetation and Its Climate Response in Arid Central Asia. *Remote Sens.* **2022**, *14*, 5922. [CrossRef]
13. Wang, L.X.; Shi, Y.L.; Zhang, H.W.; Bi, X.L.; Shen, W.M.; Ma, W.D. Analysis of Changes in Vegetation Ecological Functions and Driving Factors in the Northern Agro-Pastoral Transition Zone from 2000 to 2020. *J. Ecol. Environ.* **2021**, *30*, 1990–1998.
14. Sun, R.; Yao, P.; Wang, W.; Yue, B.; Liu, G. Assessment of wetland ecosystem health in the Yangtze and amazon river basins. *ISPRS Int. J. Geo-Inf.* **2017**, *6*, 81. [CrossRef]
15. Zheng, Y.Y.; Guo, S.T.; Su, Y. The climate boundary and its change in farming-pastoral ecotone of northern China. *Chin. J. Agric. Resour. Reg. Plan.* **2014**, *3*, 6–13.
16. Pei, H.; Liu, M.; Jia, Y.; Zhang, H.; Li, Y.; Xiao, Y. The trend of vegetation greening and its drivers in the Agro-pastoral ecotone of northern China, 2000–2020. *Ecol. Indic.* **2021**, *129*, 108004. [CrossRef]
17. Peng, Y.F.; Li, Z.Q.; Yao, X.J.; Mou, J.; Han, W.; Wang, P. Area change and cause analysis of Bosten lake based on multi-source remote sensing data and GEE platform. *J. Geo-Inf. Sci.* **2021**, *23*, 1131–1153.
18. Guo, D.; Song, X.; Hu, R.; Cai, S.; Zhu, X.; Hao, Y. Grassland type-dependent spatiotemporal characteristics of productivity in Inner Mongolia and its response to climate factors. *Sci. Total Environ.* **2021**, *775*, 145644. [CrossRef]
19. Xue, H.Z.; Chen, Y.P.; Dong, G.T.; Li, J.Y. Quantitative analysis of spatiotemporal changes and driving forces of vegetation net primary productivity (NPP) in the Qimeng region of Inner Mongolia. *Ecol. Indic.* **2023**, *154*, 110610. [CrossRef]
20. Yu, Z.W.; Miao, L.J.; Liu, Q.; Kattel, G.R.; Bao, G.; Chuai, X.W.; Zhang, Y.Y.; Zhang, H. Uncovering the impact of multiple determinants on vegetation NPP in Inner Mongolia. *Glob. Ecol. Conserv.* **2024**, *56*, e03341. [CrossRef]
21. Hao, L.; Sun, G.; Liu, Y.; Gao, Z.; He, J.; Shi, T.; Wu, B. Spatiotemporal Dynamics of Vegetation Net Primary Productivity and Its Response to Climate Change in Inner Mongolia from 2002 to 2019. *Sustainability* **2021**, *13*, 13310. [CrossRef]
22. Yao, B.; Gong, X.W.; Li, Y.L.; Li, Y.Q.; Lian, J.; Wang, X.Y. Spatiotemporal variation and GeoDetector analysis of NDVI at the northern foothills of the Yinshan Mountains in Inner Mongolia over the past 40 years. *Heliyon* **2024**, *10*, e39309. [CrossRef]
23. Yang, S.Q.; Zhao, M.; Zhang, Q.T.; Liu, X. Changes and Driving Factors of Ecological Environment Quality in the Agro-Pastoral Ecotone of Northern China from 2000 to 2020. *Land* **2025**, *14*, 2309. [CrossRef]
24. Kang, Y.; Guo, E.L.; Wang, Y.F.; Bao, Y.L.; Bao, Y.H.; Mandula, N. *Monitoring Vegetation Change and Its Potential Drivers in Inner Mongolia from* 2000 to 2019. *Remote Sens.* **2021**, *13*, 3357. [CrossRef]
25. Ren, H.R.; Shang, Y.J.; Zhang, S. Measuring the spatiotemporal variations of vegetation net primary productivity in Inner Mongolia using spatial autocorrelation. *Ecol. Indic.* **2020**, *112*, 106108. [CrossRef]
26. Wang, Y.J.; Zhang, J.Q.; Shen, X.J.; Ma, R.; Liu, Y.W.; Wu, L.Y.; Tong, S.Z.; Jiang, M.; Lu, X.G. Spatiotemporal variation of marsh vegetation productivity and climatic effects in Inner Mongolia, China. *Front. Ecol. Evol.* **2023**, *11*, 1138965. [CrossRef]
27. Yuan, M.N.; Liu, Y.X.; Wang, M.; Peng, J. Ecosystem health assessment of Guangzhou based on the framework of "vitality, organization, resilience, contribution". *Chin. J. Ecol.* **2019**, *4*, 1249–1257.

28. Xu, F.; Wang, Y.G.; Zhang, N.; Wang, X.; Fan, Q. Health assessment of watershed ecosystems: The Chao River and Bai River Basins as a case study. *Acta Ecol. Sin.* **2017**, *37*, 932–942. [CrossRef]
29. Wang, L.L.; Zhang, K.B.; Liu, X.D.; Yang, X.H. Community succession characteristics of degraded sandy grassland under enclosure management. *J. Beijing For. Univ.* **2015**, *37*, 48–54.
30. Zhao, Y.L.; Zhou, Q.P.; Zeng, L.; Dai, L.H.; Peng, Y.X.; Bai, S. A review of vegetation restoration and treatment technology for sandy grassland. *Grassl. Pratacult.* **2017**, *29*, 7–11.
31. Yue, Y.J.; Geng, L.M.; Li, M. The impact of climate change on aeolian desertification: A case of the agro-pastoral ecotone in northern China. *Sci. Total Environ.* **2023**, *859*, 160126. [CrossRef]
32. Jian, Y.Q.; Liu, Z.J.; Gong, J.Z. Response of landscape dynamics to socio-economic development and biophysical setting across the farming-pastoral ecotone of northern China and its implications for regional sustainable land management. *Land Use Policy* **2022**, *122*, 106354. [CrossRef]
33. Zhang, G.L.; Chen, X.; Zhou, Y.; Zhao, H.L.; Jin, Y.L.; Luo, Y.C.; Chen, S.Y.; Wu, X.Y.; Pan, Z.H.; An, P.L. Land use/cover changes and subsequent water budget imbalance exacerbate soil aridification in the farming-pastoral ecotone of northern China. *J. Hydrol.* **2023**, *624*, 129939. [CrossRef]
34. Shi, W.J.; Liu, Y.T.; Shi, X.L. Study on quantitative detection methods of the influence of climate change on the boundary change of the northern agro-pastoral ecotone. *Acta Geogr. Sin.* **2017**, *72*, 407–419.
35. Liu, D.; Chen, J.; Ouyang, Z. Responses of landscape structure to the ecological restoration programs in the farming-pastoral ecotone of Northern China. *Sci. Total Environ.* **2020**, *710*, 136311. [CrossRef]
36. Wei, X. Response of natural grassland NDVI to climate factors in a farming-pastoral area of Inner Mongolia. *Pratac. Sci.* **2018**, *35*, 2389–2394.
37. Zhou, L.H.; Hou, C.X. Key problems of grassland utilization and the graze ban policy in farming-pastoral ecotone of Northern China. *Arid Land Geogr.* **2019**, *42*, 354–362.

Disclaimer/Publisher's Note: The statements, opinions and data contained in all publications are solely those of the individual author(s) and contributor(s) and not of MDPI and/or the editor(s). MDPI and/or the editor(s) disclaim responsibility for any injury to people or property resulting from any ideas, methods, instructions or products referred to in the content.